



Comparative study of Eriochrome black T treatment by BDD-anodic oxidation and Fenton process

A. Bedoui^a, M.F. Ahmadi^b, N. Bensalah^{b,*}, A. Gadri^a

^a ENI-Gabes, 6029 Zrig, Gabes, Tunisia

^b Faculty of Sciences of Gabes, ISSAT-Gabes, Zrig, Gabes 6072, Tunisia

ARTICLE INFO

Article history:

Received 26 January 2008

Received in revised form 3 April 2008

Accepted 15 May 2008

Keywords:

Azoic dyes

BDD-anodic oxidation

Fenton's oxidation

Hydroxyl radicals

COD and TOC removals

ABSTRACT

In this work, the treatment of synthetic wastewaters containing Eriochrome black T (EBT) using BDD-anodic oxidation and Fenton process was investigated. The electrochemical treatment leads to almost total removal of chemical oxygen demand (COD) and total organic carbon (TOC) at different EBT initial concentrations and current densities but during Fenton reagent's oxidation of low concentrated synthetic effluents, the TOC removal reach only 75%. These results can be explained by the mechanisms involved in each process. In BDD-anodic oxidation, the influence of EBT initial concentration and current density on the evolution of COD with specific electrical charge passed shows that both direct oxidation on the surface of the electrode, and mediated oxidation by hydroxyl radicals electro-generated from water decomposition and/or by other oxidants electro-generated from sulphates ($S_2O_8^{2-}$ and SO_5^{2-}), take place and that the electrochemical process is mass-transfer controlled in the range of concentration studied. In Fenton's oxidation process, only hydroxyl radicals generated from the catalytic decomposition of H_2O_2 are able to oxidize EBT and its oxidation intermediates. The refractory carbon detected at the end of Fenton treatment can be explained by formation of stable complexes between Fe^{3+} and OH^- and/or carboxylic acids which limits the production of hydroxyl radicals. The influence of H_2O_2 and Fe^{2+} concentration on the TOC removal leads to find out the optimal conditions for obtaining the highest TOC removal at 25 °C: pH 3.5, $[H_2O_2] = 33 \text{ mg } H_2O_2 \text{ mg EBT}^{-1}$ and $[Fe^{2+}] = 6.5 \text{ mg } Fe^{2+} \text{ mg EBT}^{-1}$.

Crown Copyright © 2008 Published by Elsevier B.V. All rights reserved.

1. Introduction

Boron-doped diamond is an emergent material with good properties including great chemical, electrochemical and physical stabilities and hydroxyl radicals (OH^\bullet) formation capacity [1–3]. The production of high amounts of hydroxyl radicals lets considering BDD oxidation as an advanced oxidation process [1–5].

The use of BDD oxidation allowed obtaining high current efficiencies, which decreases strongly the operating costs of the electrochemical treatment. In the recent years, it has been widely studied for the treatment of a great variety of synthetic and real industrial wastes, both in lab and bench-scale plants [4–18]. In most cases, BDD achieved the complete mineralization of the organics contained in the wastewaters or the conversion of the toxic organics to biocompatible compounds. Possible mechanisms of the electrochemical mineralization are essentially based on oxygen-transfer stages in which electro-generated hydroxyl radicals should play a decisive role. Besides, direct oxidation on the surface and also

oxidation mediated by other oxidants electro-generated from the electrolyte salts complete the mechanism of oxidation in this kind of electrochemical technology.

Fenton process is an advanced oxidation technology in which a mixture of hydrogen peroxide and iron(II) salts is added directly to the wastewater. This mixture promotes the appearance of hydroxyl radicals by catalytic decomposition of hydrogen peroxide which gives high efficiency of the process [19–23]. In addition to the oxidation, the iron(III) ions generated during the oxidation stage promote the removal of other pollutants by coagulation and sedimentation. The Fenton's oxidation process is composed of four stages: pH adjustment, oxidation reaction, neutralization and coagulation, and precipitation. The main operation parameters of this process are the optimal ratio between H_2O_2/Fe^{2+} /organic compounds and the pH.

Dyes are colored substances are resistant to fading on exposure to light, water and many chemicals due to their complex chemical structure and synthetic origin; hence they persist in nature [24]. The discharge of dye-containing effluents into receiving waters without appropriate treatment, actually limits aquatic plant growth by creating anaerobic conditions. Most techniques used for the degradation of dyes are based on the generation of hydroxyl radicals,

* Corresponding author. Tel.: +216 75392108; fax: +216 75392404.

E-mail address: nasr.bensalah@issatgb.rnu.tn (N. Bensalah).

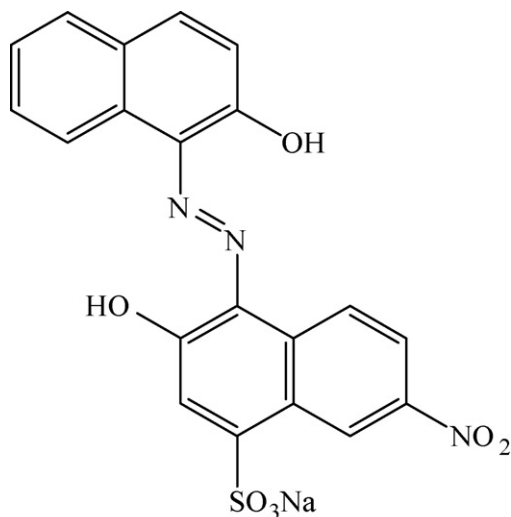


Fig. 1. Chemical structure of Eriochrome black T.

which are non-selective, very powerful oxidant agent able to react with organic until their overall mineralization [23–27]. Only few papers have raised the BDD oxidation of dyes [28–31] and especially large molecules such as Eriochrome black T (EBT), which has the chemical structure, presented in Fig. 1.

The goal of the work described here is (i) to study the treatment of synthetic wastewaters containing Eriochrome black T with BDD-anodic oxidation and Fenton process regarding the effect of various experimental parameters and operating conditions; (ii) to give more comprehensive understanding of the oxidative mechanisms in the chemical and electrochemical oxidation of organics with conductive diamond electrodes and Fenton reagent's.

2. Experimental

2.1. Chemicals

Eriochrome black T was of analytical grade and purchased from Fluka. Hydrogen peroxide was a 30% (w/w) solution (AR grade, Fluka Chemical). The other chemicals such as Na_2SO_4 , $\text{K}_2\text{Cr}_2\text{O}_7$, Na_2SO_3 , H_2SO_4 , NaOH , HgSO_4 and Ag_2SO_4 are of analytical grade and purchased from Fluka or Merck. All solutions were prepared with deionized water having $18\text{ m}\Omega^{-1}\text{ cm}^{-1}$ resistivity from a Mill-Q Trade Mark system.

2.2. Analytical procedure

The carbon concentration was monitored using Shimadzu TOC-5050 analyzer. Chemical oxygen demand (COD) was determined using a HACH DR2000 analyzer. UV-visible spectra were obtained using a Shimadzu 1603 spectrophotometer and quartz cells.

2.3. Preparation of diamond electrode

Boron-doped diamond films were provided by CSEM (Neuchâtel, Switzerland) and synthesized by the hot filament chemical vapor deposition technique (HF CVD) on single-crystal p-type Si(100) wafers ($0.1\ \Omega\text{ cm}$ Siltronise). The temperature range of the filament was $2440\text{--}2560\ ^\circ\text{C}$, and the temperature of the substrate was $830\ ^\circ\text{C}$. The reactive gas was methane in excess dihydrogen ($1\% \text{ CH}_4$ in H_2). The dopant gas was trimethylborn with a concentration of 3 mg L^{-1} . The gas mixture was supplied to the reaction chamber at a flow rate of 5 L min^{-1} , giving a growth rate of $0.24\ \mu\text{m h}^{-1}$ for

the diamond layer. The resulting diamond film thickness was about $1\ \mu\text{m}$. This HF CVD process produces, columnar, random texture and polycrystalline films with an average receptivity of $0.01\ \Omega\text{ cm}$. Prior to use in galvanostatic electrolysis assays, the electrode was polarized for 30 min with $1\text{ M H}_2\text{SO}_4$ solution at 50 mA cm^{-2} to remove any kind of impurity from its surface.

2.4. Voltammetry experiments

Electrochemical measurements were obtained using a conventional three-electrode cell in conjunction with a computer-controlled potentiostat/galvanostat (Auto lab model PGCTAT 30, Ecochemie B.V, Utrecht, The Netherlands). Diamond was used as the working electrode, $\text{Hg/Hg}_2\text{Cl}_2$ (saturated) as a reference electrode and stainless steel (AISI304) as electrode. Voltammetry experiments were performed in unstirred solutions (200 mL). The anode was anodically polarized for 5 min with a $1\text{ M H}_2\text{SO}_4$ solution at 0.1 A prior to each experiment.

2.5. Galvanostatic electrolysis

The oxidation of EBT was carried out in a single-compartment electrochemical flow cell (Fig. 2). A diamond-based material was used as the anode and stainless steel (AISI304) was used as the cathode. Both electrodes were circular (100 mm in diameter) with a geometric area of 78 cm^2 each and an electrode gap of 9 mm. The electrolyte was stored in a glass tank (500 mL) and circulated through the electrolytic cell by means of a centrifugal pump. A heat exchanger was used to maintain the temperature at $25\ ^\circ\text{C}$ by recirculation of water from a thermo-regulated bath. The experimental set up also contained a cyclone for a gas-liquid separation, as well as a gas absorber to collect the carbon dioxide contained in the gases evolved from the reaction into sodium hydroxide. The synthetic wastewaters used in the experiments contained different concentrations of EBT and 5000 mg L^{-1} of Na_2SO_4 . The cell potential was constant during each electrolysis reaction, indicating that appreciable deterioration of the electrode or passivation phenomena did not take place. The electrolyte flow rate through the cell was 1250 mL min^{-1} . The linear velocity of the fluid was 2.31 cm s^{-1} , and the space velocity was 2.08 min^{-1} .

2.6. Fenton process

Fenton oxidation assays were carried out in lab-scale thermostated mixed batch reactors. The experimental setup consists of a multistirrer device (Ikamag RO 5 power, IKA-WERKE GmbH & Co. KG, Staufen, Alemania) with fifteen mixing sites coupled with a controlled thermostatic bath (Digiterm 100, JP Selecta, Barcelona, Spain). Pyrex flasks (250 mL) hermetically sealed and equipped with magnetic stirrers were used as reactors. They were submerged in the thermostatic bath. In every assay, the reactors were filled with 100 mL of wastewater. Then, the iron dose was added (as $\text{FeSO}_4\cdot 7\text{H}_2\text{O}$) and the pH was adjusted to 3.5 ± 0.1 with sodium hydroxide or sulphuric acid. According to literature, this is the optimum pH to promote the formation of hydroxyl radicals in a Fenton process [20–22]. In every case, the reaction was started by adding the dose of hydrogen peroxide. Preliminary experiments were carried out to determine the reaction time needed to meet the steady state conditions. From these experiments a reaction time of 4 h was selected (more than three times higher than the worst value obtained in the previous experiments). Once the reaction time was finished total organic carbon (TOC), UV-visible spectra were measured in every reactor. Then, the steady state conditions were assured by a later measure (after 1 h). Several set of experiments were carried out to determine the

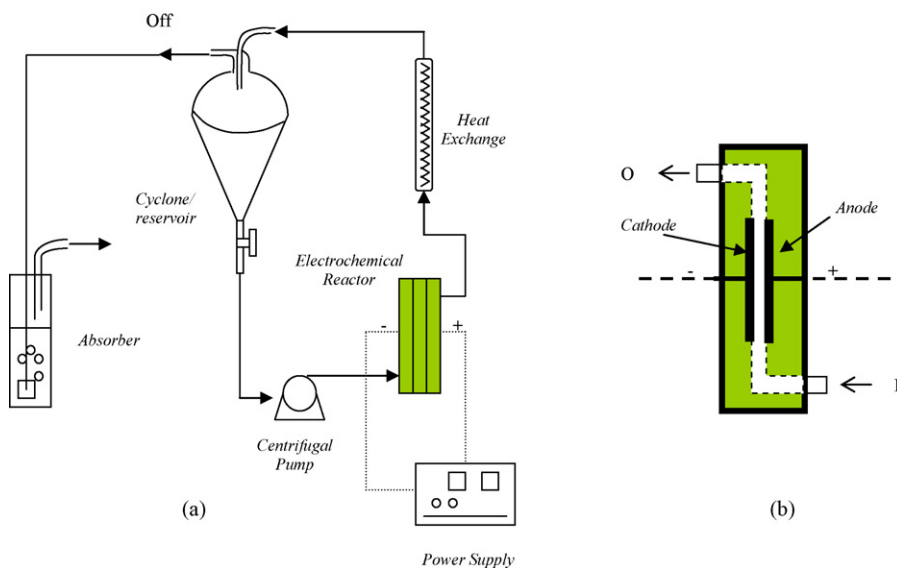


Fig. 2. (a) Experimental setup. (b) Details of the electrochemical cell.

range of hydrogen peroxide and iron needed to obtain optimum results.

3. Results and discussion

3.1. Voltammetric study

Fig. 3 shows cyclic voltammograms of aqueous solution containing EBT (100 mg L^{-1}) and Na_2SO_4 (5000 mg L^{-1}). As it can be observed, the presence of EBT leads to the appearance of an anodic oxidation peak very close to the oxygen evolution region which is partially overlapped by the side reaction. This indicates the presence of direct electron transfer between EBT and the BDD surface in the region of stability of the electrolyte. It seems that the anodic oxidation of EBT on BDD is more difficult than that of aromatic compounds [4–12]. This can be explained probably by the chemical structure of EBT which contains withdrawing groups such as NO_2 and SO_3Na . In reverse cycle, a reduction peak at -1.4 V vs. SCE is observed. This peak can be attributed to reduction of nitrogen compounds [10,11].

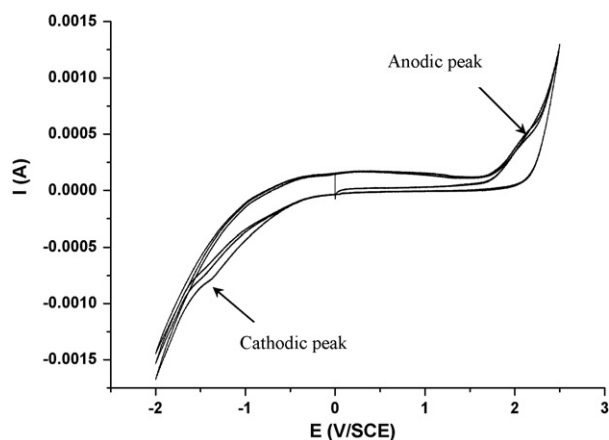


Fig. 3. Cyclic voltammograms (three consecutive cycles) on BDD anodes of EBT solutions (100 mg L^{-1}). Operating conditions: electrolyte: Na_2SO_4 5000 mg L^{-1} , pH 4.6; auxiliary electrode: platinum; reference electrode: SCE; scan rate: 100 mV s^{-1} .

On the other hand, the anodic and cathodic peaks decrease in size with the number of cycles, indicating the formation of polymers which are easily adsorbed on BDD surface. Anodic polarization at 0.1 A of BDD electrode for 5 min in $1 \text{ M H}_2\text{SO}_4$ solution, reactive the electrode surface. To explain this, it has to be taken in mind that at high anodic current densities, the oxidation of water leads to the formation of significant amounts of hydroxyl radicals [1–3]. These radicals react rapidly with the organics at the surface of the anode leading to their total mineralization and activating the surface once again. Hence, it seems clear that the EBT can be oxidized directly on the surface of the BDD in the potential region of water stability. The oxidation products of the direct oxidation of EBT lead to a deactivation of the anodic surface (probably fouling) being this problem solved working in the potential region of water oxidation.

These results suggest the oxidation of EBT, under anodic potentials between 0 and 2.5 V vs. SCE, before the water discharge, leads to the fouling of BDD anode by formation of nitrogen compounds and polymers films. This problem can be solved working in the potential region of water oxidation, where hydroxyl radicals and other oxidants formed on BDD surface, can produce the electrochemical materialization of EBT and its oxidation intermediates.

3.2. Bulk electrolysis

Galvanostatic electrolyses were carried out at constant pH 4.6 with different concentration of EBT (100 and 920 mg L^{-1}) and under two current densities (30 and 60 mA cm^{-2}).

Figs. 4 and 5 show respectively the evolution of TOC (a) and COD (b) in the electrolyte with specific electrical charge passed (Ah L^{-1}) during galvanostatic electrolyses of synthetic wastewaters containing 100 and 920 mg L^{-1} of EBT (pH 4.6, 5000 mg L^{-1} Na_2SO_4 and $j = 30 \text{ mA cm}^{-2}$). As it can be observed, the total removal of COD and the complete mineralization of the organic matter contained in the waste are achieved independently of EBT concentration. At the beginning of electrolyses, the TOC remains constant but the COD decreases which indicates that the first steps of BDD-anodic oxidation of EBT leads to the formation intermediates without CO_2 production. It should be noted that little amounts of are formed at the cathode and chemical essays confirm that these solid materials are formed by electrochemical reduction of nitroaromatics [8–11]. As it can be observed, Figs 4b and 5b show that the COD evolu-

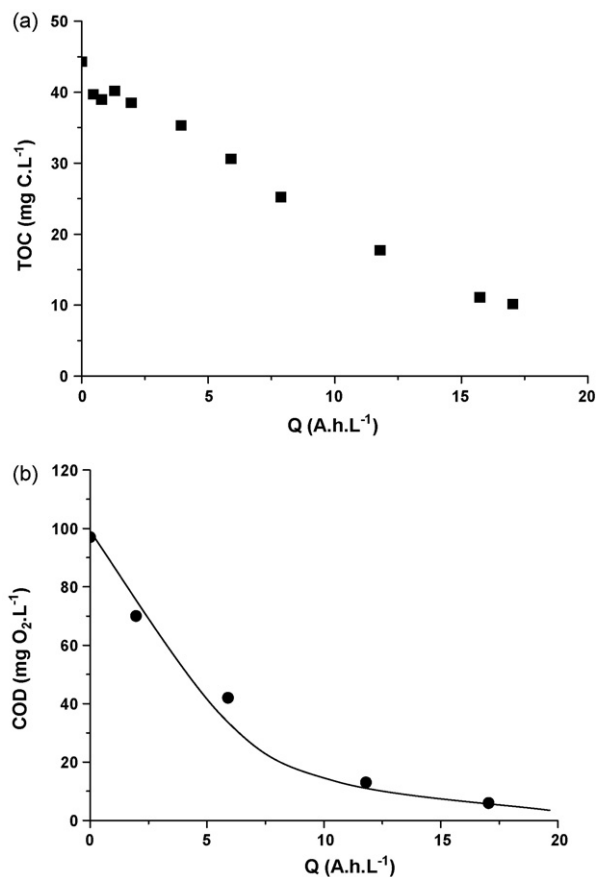


Fig. 4. Evolution of TOC (a) and COD (b) with specific electrical charge passed during the galvanostatic electrolyses of wastes polluted with 100 mg L⁻¹ of EBT. Operating conditions: 5000 mg L⁻¹ Na₂SO₄; pH 4.6; $j = 30 \text{ mA cm}^{-2}$; $T = 25^\circ \text{C}$.

tion with specific electrical charge passed have exponential shape. This is usually explained in terms of mass-transfer limitations (in the range of COD studied in this work) assuming that both direct oxidation on the BDD surface and mediated oxidation by hydroxyl radicals and other oxidants electro-generated from the supporting electrolyte (persulphates) contribute in the electrochemical process [7–11,32].

Fig. 6 shows the influence of the applied current density on the evolution of COD with specific electrical charge passed during galvanostatic electrolyses of wastewaters polluted with 920 mg L⁻¹ of EBT (pH 4.6 and 5000 mg L⁻¹ Na₂SO₄). As it can be seen, an increase in the current density does not lead to an increase in the efficiency of the oxidation process in terms of COD removal, but higher specific electrical charge are required to remove the same amount of organic matter. The COD evolution with specific electrical charge has typical exponential form. This behavior is characteristic of mass-transfer-controlled processes in which an increase in the current density cannot enhance the rate of oxidation of the organics at the electrode but favors anodic side reactions (formation of O₂, O₃, etc.) [7–11].

UV–visible spectrophotometry can give qualitative information about the discoloration rate of wastewaters polluted with EBT. Fig. 7 shows the evolution of UV–visible spectra during the electrolysis at pH 4.6 of 100 mg L⁻¹ EBT and 5000 mg L⁻¹ Na₂SO₄ solution under current density $j = 30 \text{ mA cm}^{-2}$. The initial UV–visible spectrum presents four bands at 225, 285, 340 and 540 nm. As can be observed, the intensity of the band located at visible domain (540 nm) decreases more rapidly than the others and disappears completely after 120 min indicating the total discoloration of the

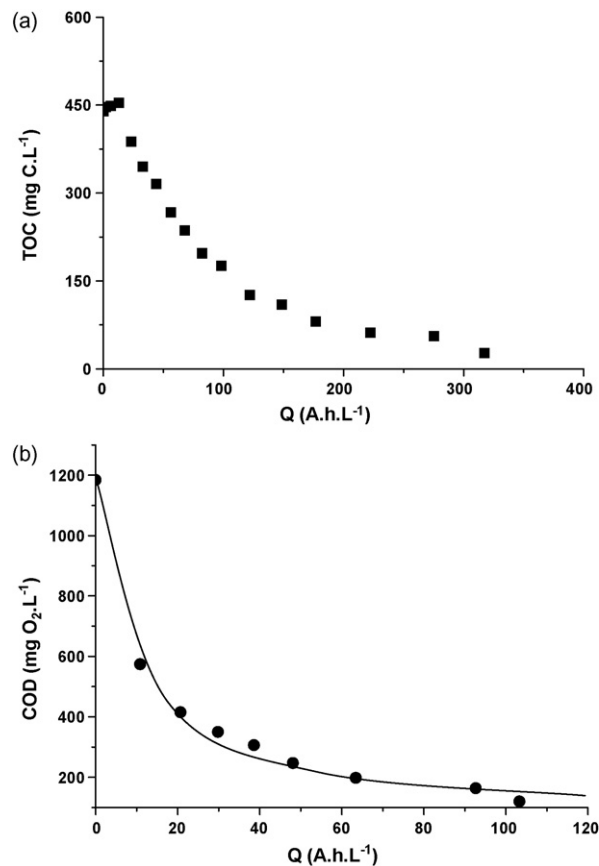


Fig. 5. Evolution of TOC (a) and COD (b) with specific electrical charge passed during galvanostatic electrolyses of wastes polluted with 920 mg L⁻¹ of EBT. Operating conditions: 5000 mg L⁻¹ Na₂SO₄; pH 4.6; $j = 30 \text{ mA cm}^{-2}$; $T = 25^\circ \text{C}$.

solution. However, the intensities the UV bands begin by increasing and after 120 min undergo continuous decrease and disappear at the end of electrolyses. These results indicate that the oxidation of this complex molecule EBT can lead to the formation of many intermediates (with decrease in the absorbance at 540 nm) by elimination of chromospheres prior to the formation carbon dioxide (that justifies the changes in the COD and TOC values previously discussed).

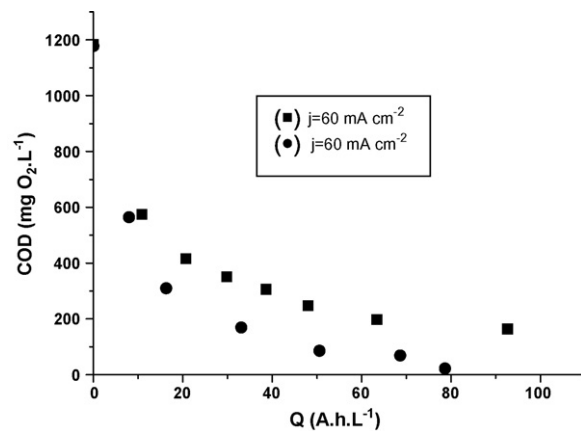


Fig. 6. Influence of the applied current density on the evolution of COD with specific electrical charge passed during galvanostatic electrolyses of wastes polluted with 920 mg L⁻¹ of EBT. Operating conditions: 5000 mg L⁻¹ Na₂SO₄; pH 4.6; $T = 25^\circ \text{C}$; current density: $j = 30 \text{ mA cm}^{-2}$ (●) and $j = 60 \text{ mA cm}^{-2}$ (■).

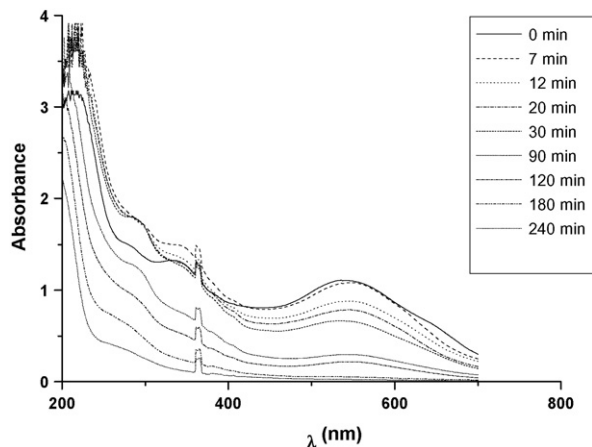


Fig. 7. Evolution of UV-visible spectra with the time during galvanostatic electrolyses of wastes polluted with 100 mg L^{-1} of EBT. Operating conditions: $5000 \text{ mg L}^{-1} \text{ Na}_2\text{SO}_4$; pH 4.6; $j = 30 \text{ mA cm}^{-2}$; $T = 25^\circ \text{C}$.

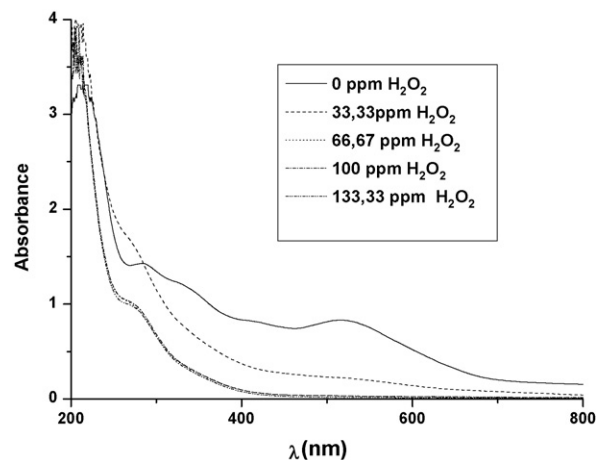
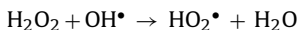
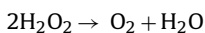


Fig. 9. Evolution of UV-visible spectra with H_2O_2 concentration during Fenton oxidation of wastes polluted with 92 mg L^{-1} of EBT. Operating conditions: $200 \text{ mg L}^{-1} \text{ Fe}^{2+}$; pH 3.5; $T = 25^\circ \text{C}$; experiment-time: 4 h.

3.3. Fenton's oxidation

The sets of runs were performed in a batch reactor to study the effect of the H_2O_2 and Fe^{2+} concentrations on the Fenton's oxidation of ERB.

Fig. 8 represents the evolution of the TOC with the H_2O_2 concentration (in mg L^{-1}) for Fenton treatment using 200 mg L^{-1} of Fe^{2+} of solutions containing 92 mg L^{-1} of EBT at pH 3.5 during 4 h. As it can be seen, the TOC decreases with increasing initial H_2O_2 concentration. When H_2O_2 concentration becomes higher than 3000 mg L^{-1} , no significant change is observed in TOC removal. To explain this, it has to be taken in mind that the increase in H_2O_2 concentration above the concentration required for the maximum TOC removal leads to a competition between the auto-decomposition of H_2O_2 into O_2 and H_2O and the scavenging of hydroxyl radicals by H_2O_2 as shown by the following sequence:



The scavenging character of H_2O_2 reduces the efficiency of the treatment through the consumption of hydroxyl radicals leading to the formation of HO_2^\bullet which has a negligible contribution in

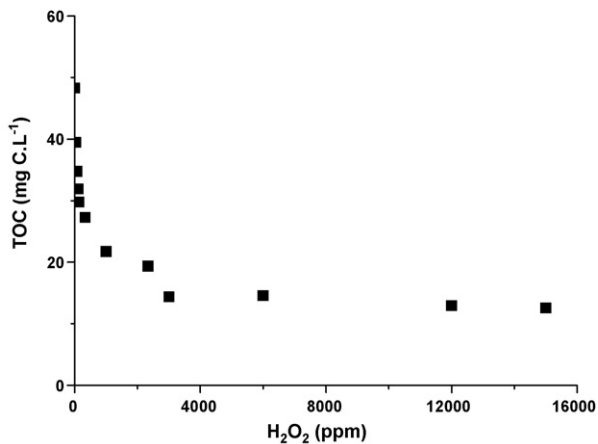


Fig. 8. Evolution of TOC with H_2O_2 concentration during Fenton oxidation of wastes polluted with 92 mg L^{-1} of EBT. Operating conditions: $200 \text{ mg L}^{-1} \text{ Fe}^{2+}$; pH 3.5; $T = 25^\circ \text{C}$; experiment-time: 4 h.

Fenton process. As it can be concluded, the required concentration of H_2O_2 for the maximum efficiency of the EBT Fenton oxidation process would be 3000 mg L^{-1} using $200 \text{ mg L}^{-1} \text{ Fe}^{2+}$ and under pH 3.5 and $T = 25^\circ \text{C}$.

UV-visible spectra for low concentration of H_2O_2 are given in Fig. 9. As it can be observed, the addition of H_2O_2 to the solution of 92 mg L^{-1} EBT and $200 \text{ mg L}^{-1} \text{ Fe}^{2+}$ at pH 3.5, leads to the disappearance of the visible band but the increase the UV bands especially the band located at 225 nm when H_2O_2 concentration is lower than 66.67 mg L^{-1} . However, for H_2O_2 concentration higher than 66.67 mg L^{-1} the UV-visible spectra are unchanged which indicates the accumulation of some intermediates such as aliphatic carboxylic acids difficult to be oxidized by hydroxyl radicals. These results indicate that using low concentrations of H_2O_2 (66.67 mg L^{-1}) during Fenton's oxidation of EBT give the total discoloration of the synthetic solutions but huge amount of H_2O_2 (3000 mg L^{-1}) is required for obtaining the maximum TOC removal. This means that the breakage of the azoic group (disappearance of visible band) can be considered as one of the first stages of the Fenton process.

In the second set of experiments pH, EBT concentration and H_2O_2 concentration were fixed respectively at 3.5, 92 and 3000 mg L^{-1} and the Fe^{2+} concentration was varied between 0 and 1500 mg L^{-1} . The experimental data concerning the variation of the TOC with Fe^{2+} concentration during 4 h are shown in Fig. 10. The TOC decreases with increasing Fe^{2+} concentration but this decrease is not significant for Fe^{2+} concentration higher than 300 mg L^{-1} . The use of high $\text{H}_2\text{O}_2/\text{Fe}^{2+}$ ratios (by weight) is recommended [31–34] because less amounts of catalyst is required without significant decrease in TOC removal and without sludge precipitation since a brown sludge was observed for Fe^{2+} concentration above 300 mg L^{-1} . The reaction time decreases with increasing the Fe^{2+} concentration indicating that high amounts of Fe^{2+} favors the elimination of organic matter by the Fenton's oxidation and coagulation because of simultaneously $\text{Fe}(\text{OH})_3$ precipitation. So high amounts of Fe^{2+} are not favorable for the treatment of ETB to avoid the problem of sludge.

The results of the first two sets of experiments show that the best initial operating conditions, for practical purpose, and for 92 mg L^{-1} EBT solution at pH 3.5 are $[\text{H}_2\text{O}_2] = 3000 \text{ mg L}^{-1}$ and $[\text{Fe}^{2+}] = 300 \text{ mg L}^{-1}$.

In the third set of experiments, the best operating conditions were used to study the evolution of TOC during the treatment. Fig. 11 shows the variation of the TOC with time during the

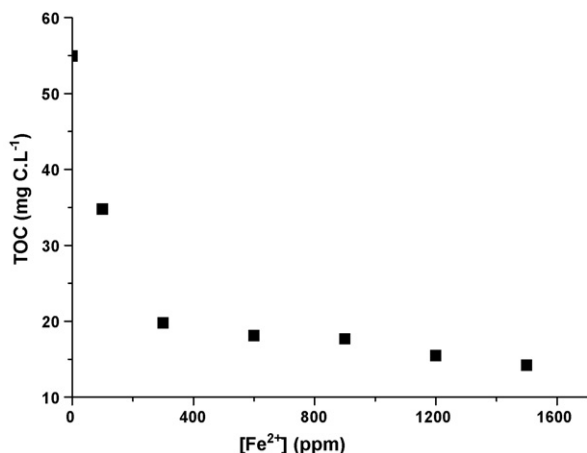


Fig. 10. Evolution of TOC with Fe^{2+} concentration during Fenton oxidation of wastes polluted with 92 mg L^{-1} of EBT. Operating conditions: $3000 \text{ mg L}^{-1} \text{ H}_2\text{O}_2$; pH 3.5; $T = 25^\circ \text{C}$; experiment-time: 4 h.

treatment of EBT solution under the best operating conditions previously mentioned. As it can be seen, the TOC decreases progressively with time leading to 75% of TOC removal after 6 h of Fenton treatment. The amounts of refractory carbon observed at the end of the Fenton treatment can be related with the difficulties found in the oxidation of aliphatic carboxylic acids by this later technique. The progressive decrease of the TOC proves the continuous formation of carbon dioxide (CO_2) during the Fenton oxidation and then the mineralization of organics contained in the waste.

On the other hand, from Fig. 11, it can be seen that the TOC removal rate is approximately constant after 240 min of the beginning of the experiment. The evolution of TOC concentration with time can be explained as follows:

- During Fenton process, the oxidation of organics is carried out with hydroxyl radicals produced by the catalytic decomposition of H_2O_2 by iron(II) with formation of iron(III) [20–22]. At the beginning of the Fenton process, high amounts of hydroxyl radicals are formed which leads to fast and continuous decrease of TOC.
- The production of hydroxyl radicals is limited by the formation of stable complexes between iron(III) and hydroxyl ions (OH^-) and/or aliphatic carboxylic acids [33,34]. This can explain the decrease in the TOC removal rate and the amounts of refractory carbon.

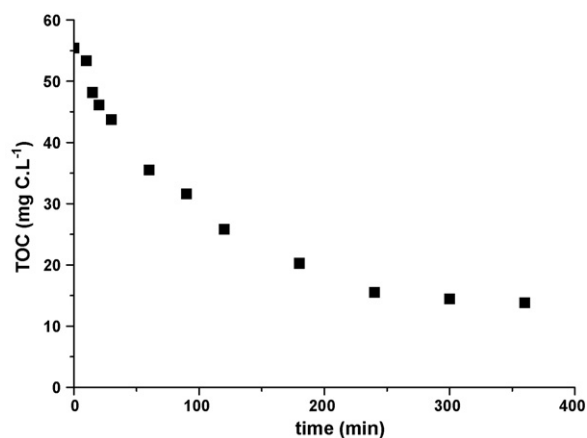


Fig. 11. Evolution of TOC with time during Fenton oxidation of wastes polluted with 92 mg L^{-1} of EBT. Operating conditions: $3000 \text{ mg L}^{-1} \text{ H}_2\text{O}_2$; $300 \text{ mg L}^{-1} \text{ Fe}^{2+}$; pH 3.5; $T = 25^\circ \text{C}$.

This part of work shows that the use of the Fenton's reagent to oxidize EBT requires a very fine control of the operating conditions. The best operating conditions can achieve only 75% of TOC removal.

According to the results obtained in this study, the BDD-anodic oxidation of wastewaters containing EBT achieves total mineralization of organic compounds using different EBT initial concentrations (low and high concentrations) and current densities. However, Fenton's oxidation of only low EBT concentrations cannot reach the total removal of TOC and amounts of refractory carbon are detected. In the BDD oxidation process, both direct oxidation on the surface of the electrode, and mediated oxidation by hydroxyl radicals electro-generated from water decomposition and/or by other oxidants electro-generated from sulphates ($\text{S}_2\text{O}_8^{2-}$ and SO_5^{2-}), of EBT take place [29–31]. In Fenton's oxidation process, only hydroxyl radicals generated from the catalytic decomposition of H_2O_2 are able to oxidize EBT and its oxidation intermediates. The BDD-anodic oxidation process produces continuously hydroxyl radicals but in Fenton's oxidation process the hydroxyl radicals production is limited by the formation of stable complexes between iron(III) and hydroxyl ions (OH^-) and/or aliphatic carboxylic acids [33,34] which can explain the detection of refractory carbon. This study shows that the BDD oxidation is more efficient than Fenton's oxidation in the treatment of complex molecule like EBT. The electrochemical oxidation on BDD anodes can be a promising technique for the treatment of wastewaters containing dyes.

4. Conclusion

The following conclusions can be drawn from the work described here:

1. Electrochemical oxidation using diamond thin film anode can be successfully used for treating aqueous EBT wastes. The total removals of the total organic carbon and the chemical oxygen demand are achieved, at different current intensities and initial EBT concentrations (within the soluble EBT range). Carbon dioxide and little amounts of easily removable solid material deposited at the cathode are the final products of the EBT oxidation by BDD-anodic oxidation.
2. Fenton's oxidation of low-loaded solutions of EBT (92 mg L^{-1}) at pH 3.5 can achieves 75% of TOC removal. Qualitative analyses obtained by spectrophotometry UV–vis show that Fenton's reagent leads to the total decoloration of the EBT solution with very low H_2O_2 concentration. The Fenton's process efficiency (TOC removal) depends largely on the H_2O_2 and Fe^{2+} concentrations. The optimal operating conditions, deduced from this work, for the treatment of synthetic waste containing 92 mg L^{-1} of EBT are: 3000 mg L^{-1} of H_2O_2 and 300 mg L^{-1} of Fe^{2+} at pH 3.5.
3. Both direct oxidation at the anode and mediated oxidation by hydroxyl radicals and other oxidants electro-generated from electrolyte oxidation are involved in the electrochemical treatment of EBT with BDD anodes [29–31]. However, only hydroxyls radicals contribute in the oxidation of EBT during Fenton process. It seems that the amounts of refractory carbon detected during the oxidation by Fenton reagent is due to formation of stable complexes between Fe^{3+} and OH^- and/or carboxylic acids [33,34] which limits the production of hydroxyls radicals.
4. The results obtained in this study suggest that BDD-anodic oxidation is more efficient than Fenton oxidation in removing TOC from solutions containing a complex molecule such as EBT.

Acknowledgement

The authors would like to acknowledge Professor Manuel A. Rodrigo (University of Castilla-La-Mancha, Spain) for his gracious assistance.

References

- [1] O. Fujio, K. Yukio, T. Hidekazu, M. Kunitake, N. Mikka, A. Toshihiro, S. Atsushi, Y. Mamoru, O. Osamu, Preparation of boron-doped semi-conducting diamond films using BF_3 and the electrochemical behavior of the semi-conducting diamond electrodes, *J. Fluorine Chem.* 125 (2004) 1715–1722.
- [2] B. Marselli, J. García-Gómez, P.A. Michaud, M.A. Rodrigo, Ch. Comninellis, Electrogeneration of hydroxyl radicals on boron-doped diamond electrodes, *Electrochem. Soc.* 150 (2003) D79–D83.
- [3] A. Kapaka, G. Foti, Ch. Comninellis, Investigations of electrochemical oxygen transfer reaction on boron-doped diamond electrodes, *Electrochim. Acta* 53 (2007) 1954–1961.
- [4] M.A. Rodrigo, P.-A. Michaud, I. Duo, M. Panizza, G. Cerisola, Ch. Comninellis, Oxidation of 4-chlorophenol at boron-doped diamond electrodes for wastewater treatment, *J. Electrochem. Soc.* 148 (2001) D60–D63.
- [5] J. Iniesta, P.A. Michaud, M. Panizza, G. Cerisola, A. Aldaz, Ch. Comninellis, Electrochemical oxidation of phenol at boron-doped diamond electrode, *Electrochim. Acta* 46 (2001) 3573–3578.
- [6] P. Cañizares, C. Sáez, J. Lobato, M.A. Rodrigo, Electrochemical oxidation of polyhydroxybenzenes on boron-doped diamond anodes, *Ind. Eng. Chem. Res.* 43 (2004) 6629–6636.
- [7] B. Nasr, G. Abdellatif, P. Cañizares, C. Sáez, J. Lobato, M.A. Rodrigo, Electrochemical oxidation of hydroquinone, resorcinol, and catechol on boron-doped diamond anodes, *Environ. Sci. Technol.* 39 (2005) 7234–7239.
- [8] P. Cañizares, J. Lobato, R. Paz, M.A. Rodrigo, C. Sáez, Electrochemical oxidation of phenolic wastes with boron-doped diamond anodes, *Water Res.* 39 (2005) 2683–2699.
- [9] P. Cañizares, J. García-Gómez, C. Sáez, M.A. Rodrigo, Electrochemical oxidation of several chlorophenols on diamond electrodes. Part I. Reaction mechanisms, *J. Appl. Electrochem.* 33 (2003) 917–927.
- [10] N. Bensalah, A. Gadri, Electrochemical oxidation of 2,4,6-trinitrophenol on boron-doped diamond electrodes, *J. Electrochem. Soc.* 152 (2005) D113–D116.
- [11] P. Cañizares, C. Sáez, J. Lobato, M.A. Rodrigo, Electrochemical treatment of 4-nitrophenol aqueous wastes using boron doped diamond anodes, *Ind. Eng. Chem. Res.* 43 (2004) 1944–1949.
- [12] E. Brillas, M.A. Baños, M. Skoumal, P.L. Cabot, J.A. Garrido, R.M. Rodríguez, Degradation of the herbicide 2,4-DP by anodic oxidation, electro-Fenton and photoelectro-Fenton using platinum and boron-doped diamond anodes, *Chemosphere* 68 (2007) 199–209.
- [13] W. Kong, B. Wang, H. Ma, L. Gu, Electrochemical treatment of anionic surfactants in synthetic wastewater with three-dimensional electrodes, *J. Hazard. Mater.* (2006) 55–68.
- [14] P. Cañizares, R. Paz, C. Sáez, M.A. Rodrigo, Electrochemical oxidation of wastewaters polluted with aromatic and heterocyclic compounds, *J. Electrochem. Soc.* 154 (2007) E165–E171.
- [15] P. Cañizares, R. Paz, C. Sáez, M.A. Rodrigo, Electrochemical oxidation of alcohols and carboxylic acids with diamond anodes. A comparison with other advanced oxidation processes, *Electrochim. Acta* 53 (2008) 2144–2153.
- [16] M. Panizza, A. Kapalka, Ch. Comninellis, Oxidation of organic pollutants on BDD anodes using modulated current electrolysis, *Electrochim. Acta* 53 (2008) 2289–2295.
- [17] A.M. Polcaro, A. Vacca, M. Mascia, S. Palmas, R. Pompei, S. Laconi, Characterization of a stirred tank electrochemical cell for water disinfection processes, *Electrochim. Acta* 52 (2007) 2595–2602.
- [18] P. Cañizares, L. Martínez, R. Paz, C. Sáez, J. Lobato, M.A. Rodrigo, Treatment of Fenton-refractory olive-oil-mills wastes by electrochemical oxidation with boron doped diamond anodes, *J. Chem. Technol. Biotechnol.* 81 (2006) 352–358.
- [19] D.R. Grymonpré, A.K. Sharma, W.C. Finney, B.R. Locke, The role of Fenton's reaction in aqueous phase pulsed streamer corona reactors, *Chem. Eng. J.* 82 (2001) 189–207.
- [20] Y.W. Kang, K.Y. Hwang, Effects of reaction conditions on the oxidation efficiency in the Fenton process, *Water Res.* 34 (2000) 2786–2790.
- [21] E. Chamarro, A. Marco, S. Espulgas, Use of Fenton reagent to improve organic chemical biodegradability, *Water Res.* 35 (2001) 1047–1051.
- [22] F.J. Rivas, F.J. Beltran, J. Frades, P. Buxeda, Oxidation of *p*-hydroxybenzoic acid by Fenton's reagent, *Water Res.* 35 (2001) 387–396.
- [23] M.A. Behnajady, N. Modirshahli, F. Ghanbary, A kinetic model for the decolorization of C.I. Acid Yellow 23 by Fenton process, *J. Hazard. Mater.* 148 (2007) 98–102.
- [24] E. Forgacs, T. Cserhati, G. Oros, Removal of synthetic dyes from wastewaters: a review, *Environ. Int.* 30 (2004) 953–971.
- [25] M. Perez, F. Torrades, X. Domenech, J. Peral, Fenton and photo-Fenton oxidation of textile effluents, *Water Res.* 36 (2002) 2703–2710.
- [26] I. Arslan-Alaton, I.A. Bacioglu, D.W. Bahnemann, Advanced oxidation of a reactive dye bath effluent: comparison of O_3 , $\text{H}_2\text{O}_2/\text{UV-C}$ and $\text{TiO}_2/\text{UV-A}$ processes, *Water Res.* 36 (2002) 1143–1154.
- [27] J. Carriere, P. Jones, A. Broadbent, Decolorization of textile dye solutions, *Ozone Sci. Eng.* 15 (1993) 189–200.
- [28] A. Fernandes, A. Morao, M. Magrinho, A. Lopes, I. Goncalves, Electrochemical degradation of C.I. acid Orange 7, *Dyes Pigments* 61 (2004) 287–296.
- [29] P. Cañizares, A. Gadri, J. Lobato, N. Bensalah, M.-A. Rodrigo, C. Sáez, Electrochemical oxidation of azoic dyes with conductive-diamond anodes, *Ind. Eng. Chem. Res.* 45 (2006) 3468–3473.
- [30] M. Faouzi, P. Cañizares, A. Gadri, J. Lobato, N. Bensalah, R. Paz, M.A. Rodrigo, C. Sáez, Advanced oxidation processes for the treatment of wastes polluted with azoic dyes, *Electrochim. Acta* 52 (2006) 325–331.
- [31] M.F. Ahmadi, N. Bensalah, A. Gadri, Degradation of anthraquinone dye alizarin red S by electrochemical oxidation on boron doped diamond, *Dyes Pigments* 73 (2007) 86–89.
- [32] P.-A. Michaud, E. Mahé, W. Haenni, A. Perret, Ch. Comninellis, Preparation of peroxodisulfuric acid using boron-doped diamond thin-film electrodes, *Electrochem. Solid State Lett.* 3 (2000) 77–80.
- [33] Y. Zuo, J. Hoigné, Formation of hydrogen peroxide and depletion of oxalic acid in atmospheric water by photolysis of iron(III)-oxalate complexes, *Environ. Sci. Technol.* 26 (1992) 1014–1022.
- [34] Y. Sun, J.J. Pignatello, Photochemical reactions involved in the total mineralization of 2,4-d by iron(3+)/hydrogen peroxide/UV, *Environ. Sci. Technol.* 27 (1993) 304–310.